

Estimating Surface Water Speeds using Time-Frequency Analysis

P. R. Kersten, R. W. Jansen, T. L. Ainsworth, J. V. Toporkov, M. A. Sletten

The Naval Research Laboratory
Remote Sensing Division, Code 7200
Washington, DC USA 20375

ABSTRACT

Joint Time-Frequency Analysis (JTFA) can estimate the speed of moving targets in Synthetic Aperture Radar (SAR) images. These targets are usually solid targets. JTFA estimation of water surface speeds is more difficult since the returns are generated by Bragg scattering epochs that are randomly distributed in the radar's footprint – in both time and space. The spectral characterization of these returns depends strongly on the geometry of the collection, which also affects the techniques needed to estimate the speeds. A novel phase differencing technique is presented to measure the frequency offset caused by the range motion of the surface water. JTFA is applied after extensive filtering to extract the motion induced component of the phase signal.

Index Terms—Time-Frequency, Joint Time-Frequency Analysis, SAR, surface water speed estimation.

1. INTRODUCTION

SAR river returns are generally weak and distributed, since they are caused by Bragg reflections from ripples or wavelets on the surface. Time-Frequency (TF) based speed estimates depend on estimating both the Doppler frequency offset and the chirp rate of the returned signal. Given a solid target moving at a constant speed with known trajectory, TF methods can estimate the velocity of the target using standard TF representations (TFRs) such as the Wigner-Ville Distribution [1-3]. In contrast, TFRs from surface water produce noisy multi-frequency-line images with weak chirp signatures and low chirp rates – especially so if the antenna beam width is small. So along with the TFRs, classical and modern spectral estimation techniques are needed to characterize and estimate the surface speeds. This paper discusses how the collection geometry determines the spectra expected from a moving target and what techniques best extract the pertinent features. Next, the X-Band NRL WINSAR Along Track Interferometric (ATI) SAR that collected our data is described along with the geometry of the collection. The data is used to illustrate the difficulties in

extracting speed estimates and the role JTFA plays. Lastly, the conclusions are presented.

2. THE IMPACT OF COLLECTION GEOMETRY

There are three cases of particular interest here. In the first case, the water flow is in range direction and then the frequency shift caused by the river flow should be proportional to the river speed. In the second case, the channel flow is across-range, which should produce no frequency shift but should produce a chirp whose rate is proportional to the speed of the river. The third case is a mixture of the first two cases. The features of interest are the frequency offset and chirp rate. The geometry is a strip mode collection and the equations that capture the frequency changes of a moving target are given by Chen [2]. The key equations are the frequency offset and chirp rate given respectively as:

$$F_c = -2(x_0V_x + y_0V_y)/\lambda R_0 \quad (1)$$

$$CRate = -2(V_x^2 + V_y^2 + x_0a_x + y_0a_y - 2V_{sar}V_x)/\lambda R_0 \quad (2)$$

In this notation, x is in the azimuth direction (cross-range) and y is in the range direction and R_0 is the distance to the scene center or initial position of the moving target (see Fig. 1 of [2]). The target velocity and acceleration terms in the x and y directions are respectively: V_x, V_y, a_x, a_y . These equations are dependent on the sign conventions used to in the image formation processing. The computations that are discussed all occur in the slow-time azimuth lines in the range-compressed image.

In the first case, $V_x = 0$ and a constant range velocity produces two frequency changes. The first is an offset, which is approximately $-2V_y y_0 / R_0 \lambda = -2V_y \cos(G) / \lambda$, where G is the grazing angle. The second is a chirp with rate $2V_y^2 / \lambda R_0$, which is small for the target velocity and slant range. All the spectral estimation techniques can be used to estimate this target induced frequency offset. In the second case, $V_y = 0$ and provided the squint is near zero,

the dominant chirp rate term of (2) is $-4V_{sar}V_x/\lambda R_0$. In theory, the TF methods should be able to detect and measure the linear FM chirp rate to estimate the azimuth velocity. In the third case, one has both a step and ramp in frequency to detect and estimate both the range and azimuth velocity.

3. THE DATA SET

The WINSAR system is a X-Band 9.7GHz ATI SAR with a Pulse Repetition Frequency (PRF) near 2 KHz. The strip-mode data-collection geometry has a 3.3 degree positive (forward) squint. The Doppler is not centered, so the signal is cut from the azimuth line in the range compressed image and windowed. It is then centered and re-embedded in an array with the original length. In addition, because the water returns are weak, the data is down-sampled by a factor of two to increase the signal-to-clutter ratio (SCR) with a corresponding decrease in the PRF. Since the antenna beam width of the WINSAR system is only 3 degrees, it is easy to manually determine the center of the signal for the azimuth lines. The data set described was not collected for research in river flow. The slant range was 2Km with an aircraft speed of approximately 90m/s. Fig. 1 contains the SAR image. The aircraft is moving from left-to-right with the near range at the bottom of Fig. 1. The image

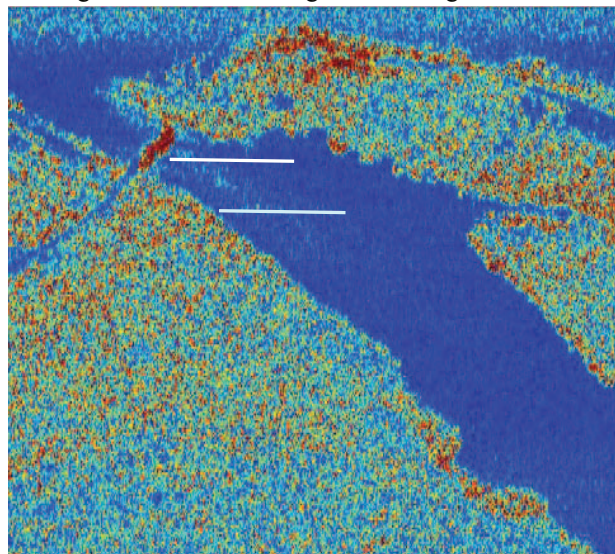


Fig. 1. The SAR image of the estuary inlet.

is an estuary located near Forfar Field Station in the Bahamas. The mouth of the estuary is in the upper-left of the image with a bridge over the narrowest part. Since the image was an opportunistic gathering, the flow rate is unknown although the tide-tables indicate the inlet is nearing high tide, so the flow should be inward at a slow rate. Slow flow rates mean weak chirp rates and small Doppler shifts due to range motion. The geometry suggests case three, so one should be able to detect both a frequency shift and a chirp. Note the streak of strong returns just after

the bridge, which seems to divide the flow – perhaps because of bridge supports. Fig. 2 shows a Google Earth image of the estuary inlet – perhaps with outward flow. One can see two channels with a quiescent region in between. This is mirrored in the SAR image. Further south into the estuary, the two streams appear to converge.

4. SIGNAL PROCESSING

Considerable signal processing is needed to extract the motion information from the water flow, which resides in the azimuth lines of the range compressed image. However, for this data set, the induced phase effects are too weak to be seen directly. Fienup suggested taking the phase differences and extracting the slope information of the signal by considering this to be a constant signal buried in noise [4]. In our case this was not feasible because the low SCR and the phase wrapping cause an ambiguity that is difficult to remove. However, the wrapping epochs proved to be a feature that was far more valuable. If only a constant speed



Fig. 2. The Google Earth estuary image – flow outward.

azimuth motion is present, then the induced phase signal is a saw-tooth where the phase wraps represented the passage of 2π radians in phase [5]. Differencing the phase term yields a constant term due to the slope of the saw-tooth and a series of the phase jumps caused by the wraps. Provided one can remove the jumps due to the phase wraps, one could use Fienup's technique. As mentioned above, we could not unwrap or reliably detect the shift in mean. Moreover, there was more than one azimuth velocity since the moving target is not a localized hard target. However, the sequence of phase wraps may be considered as a Dirac Comb (Shah function, picket fence), which when transformed is also a Dirac Comb. If one can detect this signal, then one has a measure of the frequency step caused by the range motion of the target. Since differencing the signal introduces an emphasis on the higher frequency, the phase difference was windowed and low-pass filtered. The frequency cutoff was

determined by the known speed range for the inlet. At this point a prior information is being used. The maximum speed was set at 5 m/sec even though the WINSAR ATI system gave an estimate of the range velocity of 0.6 m/sec. Any power spectral estimate of this signal may be scaled and interpreted as a distribution of range velocities. In addition, any time frequency representation (TFR) such as the short-Time Fourier Transform (STFT) can be interpreted as a variation of the velocity along the sample. Both of these effects were seen, after the filtering described above. Fig. 1 is the down-sampled image generated from the complex image data. This drops the sampling rate to approximately 1000 Hz. The azimuth offset due to the motion of the river is approximately 20 meters, which translates to approximately 200 azimuth bins. The azimuth shift [4,6] does not push the image information onto the banks, which would indeed complicate the problem.

Taking the dominant terms from both (1) and (2) one obtains an equation relating the flow speed in the azimuth direction to the frequency shift. The form of the equation is $\Delta f = V_x(A\Delta t + B)$ where Δf is the expected number of cycles received in time interval Δt , and V_x is the azimuth flow speed. The term A represents the average chirp rate and B incorporates the proportion of the range velocity generated by azimuth flow for this geometry. Since V_x is proportional to Δf , the azimuth velocity is the scaled power spectral density (PSD).

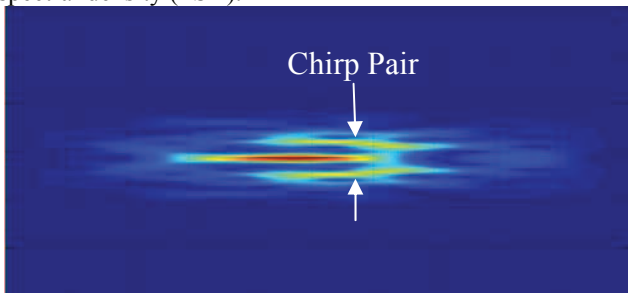


Fig 3. The STFT of an azimuth segment of the estuary inlet.

The PSD was generated directly from the correlation function using the discrete cosine transform (DCT). Any PSD estimator could be used, but this method was chosen to better understand the data. The PSD give an estimate of the frequency step and thus the average azimuth speed. The STFT of the filtered phase gives an indication of the time variation of the speed along the azimuth line.

As an example, a 512 sample was taken along an azimuth line starting from the bridge between the two inlet flow streams. The speed profile along this line should be go from low to high and back to low as it crosses the incoming stream from the inlet channel under the bridge. Fig. 3 shows the STFT, with time increasing from left-to-right and frequency increasing from top-to-bottom with the center frequency representing zero. Since the filtered phase time series is real, the higher speeds appear as a “chirp pair”

decreasing in frequency as the stream approaches the shore. The wider the pair the faster the water flow, so the pair show the speed of the stream increases sharply and gradually decrease going from left-to-right in the image. The red low frequency term is a result of the show-moving water on the left side of the stream. The white line just below the bridge at the inlet in Fig. 1, shows the azimuth line used to generate the STFT shown in Fig. 3. The left and right parts of Fig. 3 show for quiescent water the returns a very weak.

The PSD shown in Fig. 4 illustrates the distribution of speeds. In this case, the low frequency peak is the quiescent water to the left of the fast moving in put stream. The double peak at the center represents the fast moving incoming stream from the bridge, corresponding to a speed of approximately 1 m/sec.

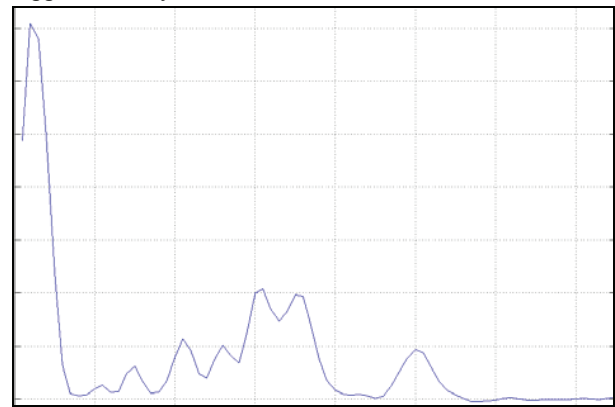


Fig. 4. The PSD for the filtered phase angle.

The fractional Fourier transform (FrFT) is also useful in displaying the variation of the flow speed [7]. The FrFT is thought of as calculating the FFT at an angular slice in the TF plane. Each slice corresponds to a different chirp rate.

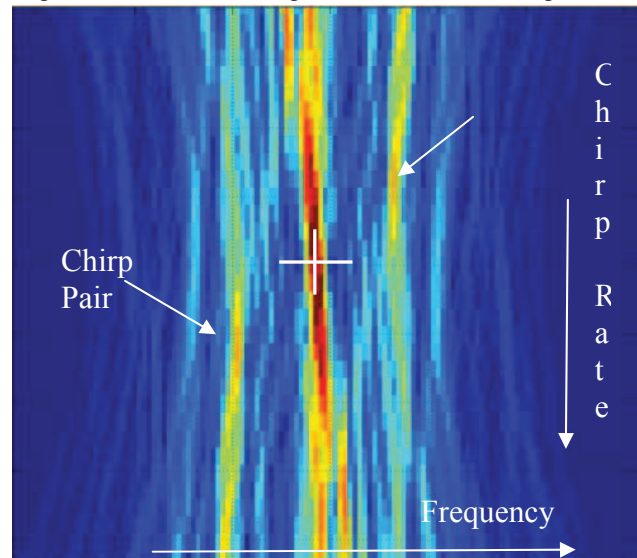


Fig 5. The chirp rate versus the frequency.

Hence, when aligned with a linear FM chirp, its response is like the FFT of a DC signal. So by collecting the FrFT for varying chirp rates into an image, one can display the chirp rates associated with differing frequency components. Fig. 5 is a plot of chirp rate vs frequency. Each chirp rate represents a different FrFT. The zero frequency and zero chirp rate are located in the center of the image with frequency along the abscissa (increasing left-to-right) and chirp rate located on the ordinate (increasing top-to-bottom). A pure linear FM chirp with rate α at center frequency f will appear concentrated in a pixel associated with that rate and frequency. For the signal illustrated in Fig. 2-3, the two yellow chirp rates in Fig. 5 are of differing signs, which is consistent with the yellow chirp pair seen in Fig. 3 and the double peak seen in Fig. 4. The chirp pair, characteristic of varying real sinusoid, indicates that the speed is slowing at the right edge of the input stream as it approaches the shore.

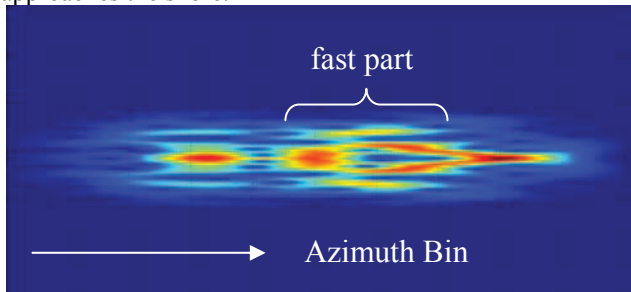


Fig 6. The STFT across converged stream in the estuary.

Further into the estuary, the two incoming streams merge into one. The second line drawn on Fig. 1 shows the azimuth segment used to construct the STFT shown in Fig. 6. The varying speeds are evident as the 0.5K azimuth segment cuts across the stream. Again, the STFT gives a good indication of the speed profile across the estuary. The fast part is in the center. The transition to slower speeds at the right edge of the stream is most clearly evident as the chirp pair converges to a single line. For this azimuth line, the PSD mean speed estimate is around 0.6 m/sec, which is consistent with WINSAR estimate of the estuary speed.

5. CONCLUSIONS AND FUTURE RESEARCH

In this paper, a novel approach for estimating surface water speed was presented. It keys upon detecting the phase wraps induced in the return signal instead of directly trying to estimate the frequency offset or chirp rate. The technique requires a priori information bounding the flow speed and the geometry of the collection. The signal filtering and windowing is essential to extract the phase information. Once the signal has been preprocessed, TF techniques can be applied to extract the spatial variations of the speed.

The results presented in this paper are preliminary and need further testing when better data becomes available. Without truth data the efficacy of these techniques is

unknown. However, we have also tested these techniques on one other data set from a C-Band Radar and have found them to work there as well.

More extensive collections are planned for the WINSAR system. So far, no river data is available to us. What is needed is an extensive collection of moving water – rivers, sea channels, estuaries, etc. In particular what is needed is multiple runs made at various directions, e.g. along the flow direction, across flow direction and at several other angles to the flow direction. Truth data is also needed, including flow rates and wind conditions. Since the SCR seems to be critical, the wind conditions which generate the Bragg reflections may determine the collection success, especially for wide slowly moving water flows. The flight path direction may be critical as well since offsets induced in the image due to the range velocity may push the returns onto a river bank or a channel shore. If banks have strong returns due to vegetation or structures, then extracting the signal may be near impossible. What is clear, that signal processing technique may be highly dependent of several factors, which suggests case-based processing and estimation techniques.

6. ACKNOWLEDGEMENTS

This work was supported in part by a grant of computer time from the DOD High Performance Computing Modernization Program at the US Army Space and Missile Defense Command Advanced Research Center. Fig. 2 was obtained from Google Earth.

7. REFERENCES

- [1] P. Kersten, R. Jansen, K. Luc, and T. Ainsworth, "Motion Analysis in SAR Images of Unfocused Objects Using Time-Frequency Methods", *Intl Geoscience & Remote Sensing Letters*, Vol 4, Issue 4, Oct, 2007, pp. 527-531.
- [2] V. C. Chen, "Time-Frequency Analysis of SAR Image with Ground Moving Targets," *SPIE*, Vol. 3391, 1998, pp. 295-302.
- [3] T.L. Ainsworth, et. al. "SAR Estimation of River Surface Currents: A sub-Aperture Analysis Approach," *IGARSS06*, pp. 2397-2399.
- [4] J. Fienup, "Detecting Moving Targets in SAR Imagery by Focusing," *IEEE TAES*, Vol 37, No 3, July 2001, pp. 794-809.
- [5] C. McGillem and G. Cooper, *Continuous and Discrete Signal and System Analysis*, Hold, Rheinart & Winston, New York, 1974, p. 112.
- [6] S. Suchandt, et. al., "Measurement of River Surface Currents using SAR Techniques," *IGARSS05*, Vol 8., pp. 5486-5489.
- [7] H. Ozaktas, "Digital Computation of the Fractional Fourier Transform," *IEEE TSP*, Vol. 44, No. 9, Sept. 1996, pp. 2141 -2150.